

wave properties (such as extremely different diffusion coefficients for the activator species) are necessary to sustain it in the area close to the antispiral core. However, generation of new waves between the basins of two adjacent antispirals does require special properties (16).

From the simple relations $R = R_0 - V_2 t$ and $\theta - \theta_0 = V_1 t / (2\pi R_0)$, where θ is the angular position measured in radians, θ_0 is an initial angle, and R is the distance from the center ($\theta - \theta_0 > 0$, $R > 0$), the equation for an inwardly rotating spiral can be deduced. For simplicity, we assume that, as a result of dispersion relations and curvature effects, V_2 is linearly dependent on the radius, so that $V_2 = V_c + R(V_0 - V_c)/R_0$, where V_c and V_0 are the velocities at the center ($R = 0$) and at $R = R_0$, respectively. Combining these three relations to eliminate the time, we obtain

$$R = R_0 [1 - a(\theta - \theta_0)] / [1 + (b - a)(\theta - \theta_0)] \quad (2)$$

where $a = V_c/V_1$ and $b = V_0/V_1$. Comparison between Eq. 2 and a simulated spiral for the case $a = b$ is shown in Fig. 3A. In Table 1, we compare the characteristic features of spirals and antispirals.

Examples of inwardly rotating spirals may be found in hydrodynamics and in Newtonian mechanics. Water funnels and the trajectory of a rotating body attracted by a large mass are simple examples of inward spirals. Inwardly propagating, but nonrotating, spiral cracks were obtained recently by drying an aqueous suspension of precipitate (23). Spirals may be classified according to whether they grow from the center or from the periphery. In outwardly rotating spirals, such as those in the aqueous BZ reaction, the point of growth is the center, the tip of the spiral. The direction of spiral propagation provides a second criterion for spiral classification. In spiral cracks, the growing point is also the tip of the spiral, but in this case the spiral curls up to and stops at the center. Peripheral spiral growth occurs, for example, in mollusc shells (nonrotating three-dimensional spirals) and in our case of rotating two-dimensional antispirals. In marine shells, the lime arms of the spiral neither move nor disappear, and therefore the spiral shell grows out from the center. In antispirals, the waves propagate in toward the center, and the peripheral growth is compensated by wave annihilation in the core. Thus, although antispirals may appear to contradict our usual notions about spiral waves, they actually fit neatly into the family of spiral behaviors. What is remarkable in the present system is how easily the type of spiral can be changed by a small variation in the structure of the microemulsion or in the chemical composition.

Two examples are known of inwardly propagating circular waves in related systems. Under some conditions, aggregating *D.*

discoideum amoebae generate patterns that look like inward concentric waves, although it is the outwardly moving waves of cAMP that drive the system (13). A second example is found in the ring-shaped pulsating waves of inhibition (reducing waves) seen by Marek *et al.* (24) in the BZ reaction. It seems likely that antispirals occur in living heterogeneous systems, such as brain tissue, heart muscle, or colonies of microorganisms, where spiral behavior has already been observed.

References and Notes

1. A. T. Winfree, *Science* **175**, 634 (1972).
2. A. N. Zaikin, A. M. Zhabotinsky, *Nature* **225**, 535 (1970).
3. K. Agladze, V. I. Krinsky, *Nature* **296**, 424 (1982).
4. K. Agladze, J. P. Keener, S. C. Müller, A. Panfilov, *Science* **264**, 1746 (1994).
5. S. C. Müller, T. Plesser, B. Hess, *Science* **230**, 661 (1985).
6. V. Pérez-Muñuzuri, R. Aliev, B. Vasiev, V. Pérez-Villar, V. I. Krinsky, *Nature* **353**, 740 (1991).
7. G. Ertl, *Science* **254**, 1750 (1991).
8. J. M. Davidenko, A. V. Pertsov, R. Salomonsz, W. Baxter, J. Jalife, *Nature* **355**, 349 (1992).
9. A. T. Winfree, *Science* **266**, 1003 (1994).
10. F. X. Witkowski *et al.*, *Nature* **392**, 78 (1998).
11. M. P. Hassell, H. N. Comins, R. M. May, *Nature* **353**, 255 (1991).
12. J. Lechleiter, S. Girard, E. Peralta, D. Clapham, *Science* **252**, 123 (1991).
13. K. J. Lee, E. C. Cox, R. E. Goldstein, *Phys. Rev. Lett.* **76**, 1174 (1996).
14. J. P. Keener, J. J. Tyson, *Physica D* **21**, 307 (1986).
15. V. S. Zykov, *Biophysics* **25**, 906 (1980).
16. V. K. Vanag, I. R. Epstein, *Phys. Rev. Lett.*, in press.
17. C. T. Hamik, N. Manz, O. Steinbock, *J. Phys. Chem. A* **105**, 6144 (2001).
18. V. I. Zarnitsina, F. I. Ataullakhanov, A. I. Lobanov, O. L. Morozova, *Chaos* **11**, 57 (2001).
19. D. Balasubramanian, G. A. Rodley, *J. Phys. Chem.* **92**, 5995 (1988).
20. V. K. Vanag, I. Hanazaki, *J. Phys. Chem.* **99**, 6944 (1995).
21. T. K. De, A. Maitra, *Adv. Colloid Interface Sci.* **59**, 95 (1995).
22. E. O. Budrene, H. C. Berg, *Nature* **376**, 49 (1995).
23. K.-T. Leung, L. Józsa, M. Ravasz, Z. Nédá, *Nature* **410**, 166 (2001).
24. M. Marek, P. Kaštánek, S. C. Müller, *J. Phys. Chem.* **98**, 7452 (1994).
25. M. Gerhardt, H. Schuster, J. J. Tyson, *Science* **247**, 1563 (1990).
26. K. J. Lee, *Phys. Rev. Lett.* **79**, 2907 (1997).
27. Q. Ouyang, J.-M. Flesselles, *Nature* **379**, 143 (1996).
28. We thank A. M. Zhabotinsky for helpful discussions. This work was supported by the Chemistry Division of the NSF.

6 July 2001; accepted 24 September 2001

Observation of Charge Transport by Negatively Charged Excitons

Daniele Sanvitto,^{1,2} Fabio Pulizzi,³ Andrew J. Shields,^{1*}
Peter C. M. Christianen,³ Stuart N. Holmes,¹
Michelle Y. Simmons,^{2†} David A. Ritchie,² Jan C. Maan,³
Michael Pepper^{1,2}

We report transport of electron-hole complexes in semiconductor quantum wells under applied electric fields. Negatively charged excitons (X^-), created by laser excitation of a high electron mobility transistor, are observed to drift upon applying a voltage between the source and drain. In contrast, neutral excitons do not drift under similar conditions. The X^- mobility is found to be as high as $6.5 \times 10^4 \text{ cm}^2 \text{ V}^{-1} \text{ s}^{-1}$. The results demonstrate that X^- exists as a free particle in the best-quality samples and suggest that light emission from optoelectronic devices can be manipulated through exciton drift under applied electric fields.

The exciton, the bound state resulting from the Coulomb attraction of an optically excited electron-hole pair, is often described as the semiconductor analog of the hydrogen atom.

¹Toshiba Research Europe Limited, Cambridge Research Laboratory, 260 Cambridge Science Park, Milton Road, Cambridge, CB4 0WE, UK. ²Cavendish Laboratory, University of Cambridge, Madingley Road, Cambridge, CB3 0HE, UK. ³High Field Magnet Laboratory, University of Nijmegen, Toernooiveld 1, 6525 ED Nijmegen, Netherlands.

*To whom correspondence should be addressed. E-mail: andrew.shields@crl.toshiba.co.uk

†Present address: School of Physics, University of New South Wales, Sydney 2052, Australia.

In 1958, Lampert (1) speculated on the existence of a class of mobile excitons, the analogs of the negative hydrogen ion (H^-) and positive hydrogen molecule (H_2^+) (2). However, because the binding energy of the second electron to the electron-hole pair is quite small, unambiguous observation (3) of a spectral line due to the negatively charged exciton (which is also called a trion) did not follow until the advent of high-quality remotely doped quantum well structures, in which the trion binding energy is substantially increased (4). This occurs at a very low excess electron density, at which each photoexcited electron-hole pair interacts with and

binds to a single excess electron (5, 6). We report direct evidence of the mobility of the negatively charged excitons by observing their drift in an electric field, which stands in contrast to the field-insensitive behavior of neutral excitons.

There has been considerable controversy about whether charged excitons can exist as the mobile, free particles Lampert originally envisaged. Indeed, it has been suggested (7, 8) that the negatively charged exciton (X^-) may be localized by the potential induced by the ionized donors in the barrier layers of the quantum well. Thus, it could be regarded as bound in a neutral complex with a barrier donor. However, there has been some indirect evidence of free X^- , such as a linear temperature dependence of its photoluminescence lifetime (9–11), as predicted for free trions (12). The question is of considerable importance, not just to herald investigations of the transport and other physical properties of a free trion, but also to form a reliable theoretical model of X^- . Such a model is required to test our understanding of the electron-electron interaction in quantum systems. The negative hydrogen ion (H^-) has been studied for many years in this regard (2). As the semiconductor analog of H^- , the negatively charged exciton allows the study of electron-electron interactions in two-, one- and zero-dimensional systems. It also facilitates investigation of two-electron physics in much larger effective electric and magnetic fields than those to which atoms can be subjected.

The most certain way to determine whether X^- is free is to observe its motion (13). We use an optical method to study the diffusion- and electric field-induced drift of X^- , and we show that in the highest quality samples, X^- is free over all the temperatures studied, whereas the X^- mobility is greatly reduced in samples with a greater degree of interface roughness.

The samples studied are two remotely doped $\text{GaAs-Al}_{0.33}\text{Ga}_{0.67}\text{As}$ quantum wells (QWs) of 100 and 300 Å thickness, grown by molecular beam epitaxy on GaAs substrates. Excess carriers were supplied to the QW by doping 2000 Å of the upper $\text{Al}_{0.33}\text{Ga}_{0.67}\text{As}$ barrier with Si donors at a concentration of 10^{17} cm^{-3} , set back from the QW by an undoped 600 Å spacer. The wafers were processed into high electron mobility transistors to allow their excess electron density to be tuned by applying a voltage between the Schottky gate and the ohmic drain contacts. For some measurements, a second bias was applied between the source and drain of the transistor, so as to induce an electric field in the plane of the QW. The samples were mounted in a variable-temperature helium flow cryostat. Photoluminescence (PL) was excited by a continuous-wave Ti-sapphire laser focused onto a 1.6- μm diameter spot on

the sample surface by a 40 \times microscope objective, creating an exciton density at the center of the laser spot of order 10^9 cm^{-2} . The emitted light was collected by the same objective, dispersed in one spatial direction by a spectrometer, and imaged onto a charge coupled device (CCD) array. Thus, the resulting image is spectrally and spatially resolved along orthogonal axes of the CCD, with resolutions of 0.1 nm and 0.7 μm , respectively.

The character of the emission from the QW is very sensitive to its excess electron density. At the negative applied gate voltage for which the quantum well is depleted of excess electrons, the PL spectrum is dominated by a sharp peak due to recombination of neutral excitons (10). In the presence of a dilute density of excess electrons, these neutral excitons are able to bind an excess electron to form negatively charged excitons, i.e., $X + e^- \rightarrow X^-$. Upon changing the gate bias to increase the excess electron density in the quantum well, we observe the neutral exciton peak weaken and another sharp peak emerge to lower energy and strengthen, due to the presence of X^- (10). Eventually, at an electron density of $\sim 2 \times 10^{10} \text{ cm}^{-2}$, all X are converted to X^- and only the X^- line remains in the PL of the quantum well. Thus, we are able to study the behavior of neutral and negatively charged excitons in the same sample simply by changing the applied gate voltage and thereby the excess electron density. We see qualitatively different drift behavior for the two species.

For all the experimental results presented here, the PL has been recorded with the laser energy very close to the energy of the emitting exciton, X or X^- (Fig. 1A). With the laser resonant to the X^- transition, we ensure that neutral excitons are not present. At low temperatures, thermally excited neutral excitons can be neglected (10). Thus, the observed spatial profile of the X^- emission can only be caused by diffusion of X^- (14).

The most unambiguous proof of the free nature of trions is their drift in an electric field. An electric field can be induced along a direction in the QW plane by applying a voltage between the source and drain of the transistor. For these measurements, the gate-drain bias, which determines the excess electron density in the QW, was fixed at a value of -0.62 V , at which only the X^- line is present in the PL spectrum (Fig. 1). Without source-drain bias, the image is symmetric (Fig. 1A), whereas the X^- emission is skewed in the opposite direction to the applied field for that taken with in-plane bias (Fig. 1B). Increasing the in-plane field leads to a more pronounced asymmetry (Fig. 1C). If the sense of the electric field is reversed, the charged excitons are observed to drift in the opposite

direction; Figure 2A compares the X^- diffusion profile of the 300 Å QW for source-drain biases of +0.1, 0.0, and -0.1 V . These observations demonstrate directly that X^- is indeed a free, negatively charged particle.

The same experiment performed on the neutral exciton (Fig. 2B) shows that, in contrast to the behavior displayed by X^- , an applied electric field (in either direction) has no effect on the X diffusion profile, which one would expect because X has no net charge. This result and the fact that we do see a drift for a charged exciton in electric field, indicates that the model of a trion formed by a free exciton hopping between localized electrons suggested in (15) cannot explain our experimental results. Furthermore, because X^- drifts like a negatively charged particle (i.e., in opposite direction to the field), the possibility that we are observing the hopping of holes in the opposite direction, which would be the case if the trion was

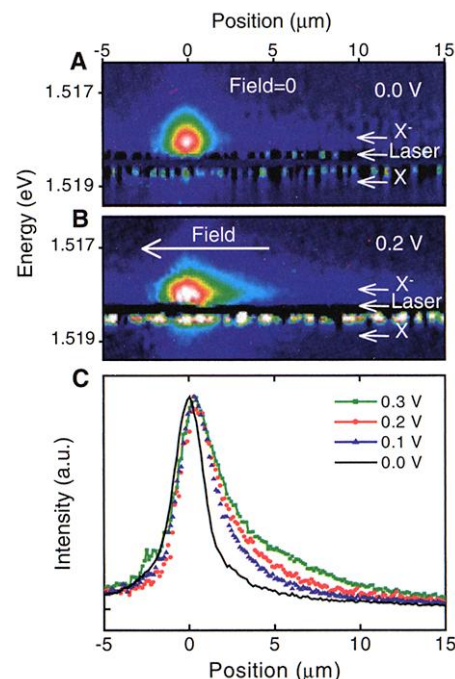


Fig. 1. The effect of an applied electric field in the plane of the QW on trion diffusion in the 300 Å QW. (A) Image of the trion PL recorded on the CCD, resolved in wavelength and one spatial direction. (B) Same as in (A), but with a voltage of 0.3 V applied between source and drain of the transistor. As in all the experiments here, the laser wavelength ($\lambda = 817.25 \text{ nm}$) is tuned close to resonance with the trion to avoid excitation of neutral excitons. (C) Trion diffusion profile of zero electric field (black solid line) and with increasing electric field (colored lines, with voltage shown in the key). One side of the diffusion profile shows an increasing broadening, due to drift of the charged trions in the electric field. As expected for a negative particle, the trions drift in the opposite direction to the field.

actually formed by a hole hopping between localized electrons, is excluded.

Further evidence for free motion of trions is given by the spatial PL profiles as a function of temperature (Fig. 3), without applied in-plane bias. For the 300 Å QW, the profile is clearly broader than the laser at 4.2 K (solid line in the figure) and broadens further upon increasing the sample temperature (Fig. 3A). For the 100 Å QW, though, the profile is much narrower but still shows a clear broadening at the highest temperatures studied. To quantify the spatial extent, we measured for each curve the width of the profile at a normalized intensity $I = I_{\text{max}}/e$ (Fig. 3C). For the 300 Å sample, the spatial extent increases from 2.9 μm at 4.2 K to 4.3 μm at 12.5 K and is always much wider than the laser spot (1.6 μm).

In order to estimate the trion mobility, we describe the data with a two-dimensional diffusion equation

$$D\nabla^2 n(x, y) + I(x, y) - \frac{n(x, y)}{\tau} = 0 \quad (1)$$

where D is the diffusion coefficient; $n(x, y)$ is the local trion concentration; $I(x, y)$ is the trion injection rate, which is assumed to be proportional to the measured laser profile; and τ is the trion lifetime. τ was measured independently by time-resolved photoluminescence spectroscopy in the 300 Å sample to be a linear function of temperature, which evolves from 177 ps at 4.2 K to 405 ps at 12.5 K (10). We have solved the equation, leaving D as the only fit parameter. A typical fitting trace is plotted in Fig. 3A for the X^- diffusion at 4.2 K ($D = 30 \text{ cm}^2/\text{s}$). As we can see, there is a very good agreement up to

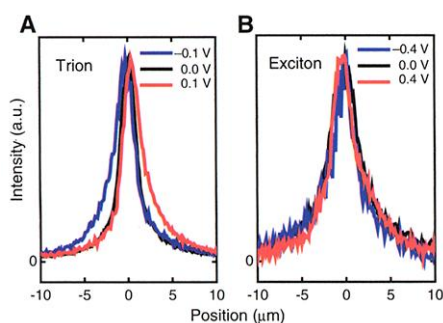


Fig. 2. Effect of reversing the electric field direction on the diffusion profile of X^- and X in the 300 Å QW sample. (A) Trion diffusion profile in the presence of an applied source-drain voltage of -0.1 V (blue line), 0.0 V (black), and $+0.1 \text{ V}$ (red). This shows that changing the electric field direction reverses the direction in which X^- drifts. (B) Neutral exciton diffusion profile recorded at very low electron density (-0.7 V) for which X dominates the PL and laser excitation is resonant with the exciton line. Application of a voltage of 0.4 V in either direction (red and blue lines) does not alter the zero field diffusion profile (black line), consistent with the neutral net charge of X .

$\sim 2 \text{ } \mu\text{m}$ from the center. Equation 1 is a simple diffusion model, which considers a homogeneous quasi-thermal distribution and a spatially constant diffusion coefficient. The unfitted tail at long distances is probably due to the fact that X^- , with larger kinetic energy, has a longer recombination time because of the decline in transition matrix element with increasing exciton wavevector. (12). However, the agreement with 80% of the profile allows us to make an estimate of the trion

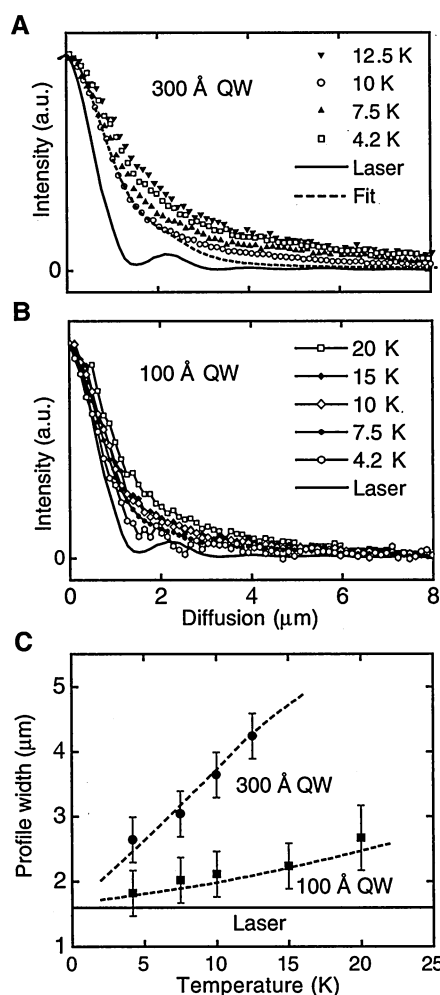


Fig. 3. Spatial diffusion of the trion emission around the laser excitation spot measured at different sample temperatures, for (A) X^- in the 300 Å QW sample and (B) X^- in the 100 Å QW. The curves are normalized to the same peak intensity. (C) Temperature dependence of the spatial extent of the diffusion profile. For the 300 Å QW, the diffusion profile is much broader than the laser profile (solid line), even at 4.2 K, and it increases with temperature. This is clear evidence that X^- is free to move in the plane of the QW, with a fitted mobility of $6.5 \times 10^4 \text{ cm}^2\text{V}^{-1}\text{s}^{-1}$. For the 100 Å QW, the trion profile is similar to the laser at the lowest temperatures, but it is clearly broader than the laser above 10 K. This indicates that the mobility of the trions in the 100 Å QW is lower. The solid lines in the figure are the spatial extents calculated using Eq. 1 and a temperature-independent mobility.

mobility $\mu = (6.5 \pm 1.0) \times 10^4 \text{ cm}^2\text{V}^{-1}\text{s}^{-1}$, using the Einstein relation $D = \mu kT/e$. The increase in extent of the emissive region with temperature (Fig. 3C) can be well described (Fig. 3C, solid line) by the simple model with the use of a mobility that is independent of temperature. The value of the trion mobility is approximately three times smaller than the electron mobility in this sample, which is measured to be $\mu = 2 \times 10^5 \text{ cm}^2\text{V}^{-1}\text{s}^{-1}$ under similar experimental conditions, reflecting the heavier trion mass compared to the electron mass. Taking an effective mass of $0.25 m_0$, where m_0 is the free electron mass, we thus deduce a transport lifetime for the trion of 9.1 ps, which is probably limited by scattering with background impurities in the GaAs channel. Using the same procedure (Fig. 3C, solid line), the X^- mobility in the 100 Å QW sample was found to be significantly lower ($\mu = 10^4 \text{ cm}^2\text{V}^{-1}\text{s}^{-1}$). We suppose that the lower X^- mobility of the 100 Å is due to the larger potential fluctuations due to interface roughness in the narrower well.

The observed spatial diffusion of negatively charged excitons away from a tightly focused laser spot demonstrates that they are free in high-quality quantum well samples. The determined mobility of $6.5 \times 10^4 \text{ cm}^2\text{V}^{-1}\text{s}^{-1}$ is relatively high for a nondegenerate gas, suggesting that the background electrons may screen the donor impurity charge. The momentum scattering time for X^- of 9.1 ps is similar to that measured for the electrons at the same electron density. As charged, free particles, trions undergo drift in an applied electric field.

References and Notes

- M. A. Lampert, *Phys. Rev. Lett.* **1**, 450 (1958).
- H. A. Bethe, E. E. Salpeter, *Quantum mechanics of one and two electron atoms* (Springer, Berlin, 1957), pp. 154–157.
- K. Kheng *et al.*, *Phys. Rev. Lett.* **71**, 1752 (1993).
- B. Stébé, A. Ainane, *Superlatt. Microstruct.* **5**, 545 (1989).
- A. J. Shields, M. Pepper, D. A. Ritchie, M. Y. Simmons, G. A. C. Jones, *Phys. Rev. B* **51**, 18049 (1995).
- A. J. Shields, M. Pepper, D. A. Ritchie, M. Y. Simmons, *Adv. Phys.* **44**, 47 (1995).
- G. Finkelstein, H. Shtrikman, I. Bar-Joseph, *Phys. Rev. Lett.* **74**, 976 (1995).
- G. Eytan, Y. Yayon, M. Rappaport, H. Shtrikman, I. Bar-Joseph, *Phys. Rev. Lett.* **81**, 1666 (1998).
- A. Ron *et al.*, *Solid State Commun.* **97**, 741 (1996).
- D. Sanvitto *et al.*, *Phys. Rev. B* **62**, 13294 (2000).
- V. Ciulin *et al.*, *Phys. Rev. B* **62**, 16310 (2000).
- A. Esser, E. Runge, R. Zimmerman, W. Langbein, *Phys. Rev. B* **62**, 8232 (2000).
- B. Stébé, G. Munsch, L. Stauffer, F. Dujardin, J. Murat, *Phys. Rev. B* **56**, 12454 (1997).
- F. Pulizzi *et al.*, *Phys. B* **298**, 397 (2001).
- G. Finkelstein, H. Shtrikman, I. Bar-Joseph, *Phys. Rev. B* **53**, 12593 (1996).
- We thank K. Cooper for his help preparing the samples.

30 July 2001; accepted 14 September 2001
Published online 27 September 2001;
10.1126/science.1064847
Include this information when citing this paper.